JOURNAL OF
biomaterials
applications

Biomaterials Processing

Journal of Biomaterials Applications
2021, Vol. 35(9) 1192–1207

DOI: 10.1177/08853282209811 89
journals.sagepub.com/home/jba
SAGE

Development of biological meniscus scaffold: Decellularization method and recellularization with meniscal cell population derived from mesenchymal stem cells

Aylin Kara[1], Semra Koçtürk[2], Gokcen Bilici[3] and Hasan Havitcioglu[4]

Abstract

Tissue engineering approaches which include a combination of cells and scaffold materials provide an alternative treatment for meniscus regeneration. Decellularization and recellularization techniques are potential treatment options for transplantation. Maintenance of the ultrastructure composition of the extracellular matrix and repopulation with cells are important factors in constructing a biological scaffold and eliminating immunological reactions.

The aim of the study is to develop a method to obtain biological functional meniscus scaffolds for meniscus regeneration. For this purpose, meniscus tissue was decellularized by our modified method, a combination of physical, chemical, and enzymatic methods and then recellularized with a meniscal cell population composed of fibroblasts, chondrocytes and fibrochondrocytes that obtained from mesenchymal stem cells. Decellularized and recellularized meniscus scaffolds were analysed biochemically, biomechanically and histologically. Our results revealed that cellular components of the meniscus were successfully removed by preserving collagen and GAG structures without any significant loss in biomechanical properties. Recellularization results showed that the meniscal cells were localized in the empty lacuna on the decellularized meniscus, and also well distributed and proliferated consistently during the cell culture period ($p < 0.05$). Furthermore, a high amount of DNA, collagen, and GAG contents ($p < 0.05$) were obtained with the meniscal cell population in recellularized meniscus tissue.

The study demonstrates that our decellularization and recellularization methods were effective to develop a biological functional meniscus scaffold and can mimic the meniscus tissue with structural and biochemical features. We predict that the obtained biological meniscus scaffolds may provide avoidance of adverse immune reactions and an appropriate microenvironment for allogeneic or xenogeneic recipients in the transplantation process. Therefore, as a promising candidate, the obtained biological meniscus scaffolds might be verified with a transplantation experiment.

Keywords

Meniscus, decellularization, recellularization, mesenchymal stem cells, fibrochondrocytes, tissue engineering

Introduction

The meniscus is a fibrocartilage structure that plays an important role in the knee joint with a function in load bearing, load transmission, shock absorption, joint stability and joint congruity.[1,2] Loss of this anatomical structure results in higher peak stresses on the cartilage, leading to cartilage degeneration and osteoarthritis.[3] In the United States, around 50% of the 1,500,000 arthroscopic knee surgeries performed annually are related to meniscus and The British Orthopedic Sports Trauma Arthroscopy Society (BOSTAA) reported that 60–70 out of 100,000 people complained of meniscal problems[4,5]

[1]Department of Bioengineering, İzmir Institute of Technology, İzmir, Turkey
[2]Faculty of Medicine, Department of Biochemistry, Dokuz Eylül University, İzmir, Turkey
[3]Faculty of Medicine, Department of Histology and Embryology, Dokuz Eylül University, İzmir, Turkey
[4]Faculty of Medicine, Department of Orthopedics and Traumatology, Dokuz Eylül University, İzmir, Turkey

Corresponding author:
Semra Koçtürk, Dokuz Eylül University, Faculty of Medicine, Department of Biochemistry, 35340, İzmir, Turkey.
Email: semra.kocturk@deu.edu.tr

Meniscus structure is composed of three distinct layers: (i) a superficial fibril network covering the femoral and tibial surfaces, (ii) a lamellar layer, (iii) a central main layer. The lamellar layer contains collagen fibrils in a radial direction and the central main region is composed of collagen fibers in a circumferential orientation.[6] The superficial fibril layer covered the tibial and femoral sides of the meniscus surface by fibrils mesh which has no specific orientation. The cell types of the meniscus are fibroblast-like cells, chondrocytes, and fibro-chondrocytes. Fibroblast-like cells are located in the peripheral region of the meniscus and respond to environmental stresses and compressive forces. The extracellular matrix (ECM) of these cells are mainly comprised of type I collagen and small percentages of glycoproteins and collagen type III and V. Second population of the cells, chondrocytes or superficial zone cells are located in the superficial zone which is synthesized a large amount of type II collagen and glycosaminoglycans (GAG). They play an important role in the healing of the meniscus by migrating to the injured area. Fibrochondrocytes, the cells of the inner region, provide contact with other cells and different parts of the matrix by synthesizing large amounts of fibrous type I and type II collagen and aggrecan.[7,8]

Generally, total meniscectomy is used to treat meniscal injury, but it leads to knee damage and osteoarthritis.[9–11] Therefore, current treatments of meniscus include partial meniscectomy and allograft transplantation to avoid osteoarthritis.[12–15] Recently, the use of ECM scaffolds by means of decellularization of allograft tissue has become the preferred application.[16–18] Although allografts or synthetic meniscus scaffolds can be used for this application, problems related to stability and immunological reactions prevent widespread clinical use.[18] In this approach, to provide mechanical strength, decellularized biological scaffolds similar to ECM are used as supportive biological structures. Therefore, to reduce immunological reactions, implantation of decellularized meniscus tissue to the recipients from a different donor is significant. However, decellularization is an important step for preventing of immunological reactions in transplantation. Different decellularization methods such as physical (high pressure, freeze-thaw cycles), chemical (anionic and nonionic detergents) and enzymatic (DNase, Trypsin,) have been used to prepare biological scaffold.[19,20] Research revealed that the antigenicity of the implanted meniscus varies depending on the used decellularization method, which directly affects the success of the treatment. To improve the long-term outcome of meniscus allografts, new decellularization strategies are needed.

The objectives of the study are to develop an effective decellularization method that protects ECM structure and recellularization with mesenchymal stem cells that mimic meniscal cell population in a short period. For these purposes, rabbit menisci were decellularized with a combination of chemical, physical and enzymatic methods with minimum chemical concentration and incubation time. Decellularized meniscus ECM structure were assessed by histological staining, biochemical and biomechanical tests. It was shown that DNA content was decreased, and ECM composition of the meniscus tissues was maintained while preserving the biomechanical properties. Following the decellularization, a meniscal cell population consisting of fibroblasts, chondrocytes and fibrochondrocytes was obtained from rabbit bone marrow derived mesenchymal stem cells (rMSCs) for recellularization of decellularized meniscus tissues. Meniscal cell populations were appropriately localized on empty lacuna in decellularized meniscus tissues and proliferated in an increasing trend. Our results revealed that combinational uses of chemical, physical and enzymatic methods provide a successful decellularization to remove the cellular components without any damage to the structure and stability of the ECM and to seed derivatized cells from MSCs that produce native meniscus allograft in a short period. Therefore, we suggest that our methods, favorable to the production of the biological meniscus scaffolds, may a promising candidate for use in transplantation.

Materials & methods

Materials

Materials used in the decellularization process include tris-HCl, sodium dodecyl sulfate (SDS), ethylene diamine tetra acetic acid (EDTA), DNase I, RNase, magnesium chloride, bovine serum albumin (BSA), and sodium chloride, which were purchased from Sigma. Hematoxylin eosin (HE) (Biooptica), Alcian blue (Ab) (Raymond A Lamb, United Kingdom), Masson trichrome (MT) (GBL, Turkey), Oil Red O staining kit (BioVision, K580-24), Collagen I (Abcam, ab90395) and Collagen II Antibody (Novus Biologicals, NBP2-33343), Aggrecan Antibody (Novus Biologicals, NB120-11570), and Anti-Vimentin antibody (Abcam, ab92547) were used for histological staining. In biochemical tests, hydroxyproline assay kit (Quickzym Biosciences), Sulfate Glycosaminoglycan Quantification Kit (Amsbio, AMS Biotechnology) and DNeasy 96 Blood & Tissue Kit (Macherey-Nagel) were used for detection of collagen, GAG and DNA content in meniscus tissues respectively. For cell culture studies, all media and supplements were purchased from Biochrome (Berlin, Germany). Besides Transforming growth factor beta (TGFβ), Insulin growth factor (IGF), basic fibroblast growth factor

(bFGF), dexamethasone, ascorbic acid, ITS+Premiks, isobutyl-metylxantine, insulin, indomethacin, and β-glycerophosphate were supplied from Sigma, and cell detachment solution and accutase were purchased from StemCell, BD. CD 73 (APC anti-rabbit IgG1), CD 90 (FITC anti-rabbit IgG1), CD 34 (PE anti-rabbit IgG1), and CD 45 (PE/Cy5.5 anti-rabbit IgG1) surface markers (Abcam) were used for flow cytometry analysis. XTT Cell Viability Kit (XTT; 2,3-bis-(2-methoxy-4-nitro-5-sulfophenyl)-2H-tetrazolium-5-carboxanilide), Cell Signaling Technology Inc.) and LDH Cytotoxicity Detection Kit (LDH; Lactate dehydrogenase, Roche) were used for cell viability and toxicity assays.

Methods

Preparation of the meniscus tissue. Twenty New Zealand White Rabbits (age, 4 months; weight, 2.5–3.0 kg; female) were obtained from Dokuz Eylul University, Department of Laboratory Animal Science (İzmir, Turkey). All animal experiments were performed in accordance with the protocol accepted by Dokuz Eylul University Experimental Animals Ethical Council (Protocol No: 95/2013). After disinfection, the medial menisci were dissected from the knee joint by gently excising the knee capsule. For all examinations, tissues were cut into two symmetrical pieces for control and sample groups in the same tissue. Tissues were stored at -20°C in PBS until further use.

Decellularization of the meniscus tissue. Decellularization was performed based on a minor modification of the procedure described by Stapleton et al.[21] Decellularization process carried out with minimum concentration of SDS without aprotinin at 14th days. Firstly, physical treatment was subjected to three freeze-thaw cycles, freezing −20°C for 4 h and thawing at room temperature for 2 h. Three more cycles with addition of hypotonic buffer solution (10 mM tris-HCl, pH 8.0) were carried out. Then chemical treatment was performed; samples were incubated in hypotonic buffer at 37°C for 24 h followed by 0.1% (w/v) SDS in the presence of 0.1% (w/v) EDTA at 45°C for 48 h with agitation. These steps were repeated as three cycles. Samples were washed in PBS twice for 12 h. Following washing, samples were incubated twice in nuclease solution consisting of DNase I (50 U/mL) and RNase (1 U/mL) in 50 mM tris-HCl and 50 mg/mL BSA buffer for 3 h at 37°C. 1.5 M NaCl in 0.05 M tris-HCl was used as a final incubation step, then samples were washed with PBS for 24 h at room temperature. For sterilization, samples were incubated 0.1% peracetic acid in PBS for 3 hours. Finally, meniscus tissues were washed two times in PBS at 37°C and 25°C for 24 h.[22]

Verification of the decellularization method

Histology. Meniscus tissues were evaluated histologically to characterization of the decellularization process. Initially, tissue samples were fixed in 10% (v/v) neutral buffered formalin for 72 h and then dehydrated using routine process before embedding in paraffin. 5 µm thick sections were prepared on slides and hematoxylin eosin (HE) staining was used to evaluate tissue histoarchitecture. Besides, Alcian blue (Ab) and Masson trichrome (Mt) staining were used to visualize GAG and collagen distribution and orientation respectively. Paraffin sections of tissues were also immunolabeled for aggrecan, vimentin, type I and type II collagen.

All tissue samples were evaluated considering red, red-white, white, and superficial zone (Figure 1).[2,23,24]

Biochemical analysis. Total DNA content of native and decellularized meniscus tissues (n = 3) was determined after the decellularization process. Firstly, meniscus tissues homogenized with DNeasy Kit, following of the manufacture's protocol, then DNA content of tissues were measured absorbance at 260/280 nm by Nanodrop spectrophotometer (Nano 2000, Labtech, Thermo Scientific).

Hydroxyproline assay was used to determine total collagen content of the tissues (n = 3). Standards and test solutions were prepared according to the Quickzym kit manual. The absorbance at 570 nm was measured (Varioskan Flash, ThermoFisher Scientific) and the concentration of hydroxyproline was estimated by interpolation from a hydroxyproline standard curve.

GAG content of the native and decellularized tissues (n = 3) was determined using the Sulfate Glycosaminoglycan Quantification Kit based on 1,9-DMMB binding. After enzymatic digestion, standard or test solution were prepared following manufacturer's protocol. The absorbance at 530 nm was measured using a microplate reader (Varioskan Flash, ThermoFisher Scientific). The resultant concentration of sulfated sugars representative of GAG was determined by interpolation from the standard curve.

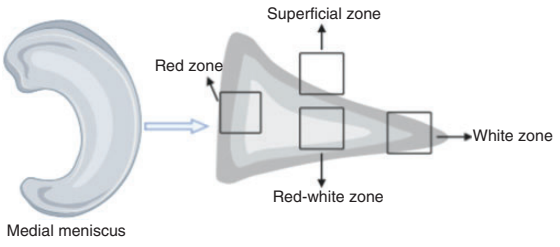

Figure 1. Red, red-white, white and superficial zone of the meniscus tissue.

Biomechanical test. Decellularized and native meniscal samples (n = 6) were cut using a 2,5 mm diameter by biopsy punch from the same location of the medial meniscus. Samples were immersed in PBS during the tests, and 5 N load was applied under axial load with electromechanical actuator (5 kN AG-X; Shimadzu, Japan). The max load (P), poison ratio (v), displacement (φ), K (K= a/h; radius of indenter (a), thickness of the samples (h)) were recorded and elasticity modulus of the tissues (E) were calculated according to the equation described below.[25]

$$E = (P(1 - v^2))/2a\varphi K \quad (1)$$

Preparation of meniscus cell population

Isolation and culture of rabbit mesenchymal stem cells (rMSCs). Rabbit bone marrow derived mesenchymal stem cells were used to obtain meniscus cell population consisting of fibroblast chondrocytes and fibrochondrocytes. rMSCs were isolated from bone marrow of New Zealand White rabbits by ficoll paque density-gradient centrifugation.[26] Cell suspension were cultured DMEM consist of 10% FBS, 1% penicillin/streptomycin/amphotericin B and 200 mM glutamine for 14 days at 37°C, 5% CO_2 and 95% humidity. The culture medium was replaced every 3–5 days, and the cells were subcultured at 90% confluence. Cells were observed under an inverted microscope during the culture period.

Flow cytometric identification of rabbit mesenchymal stem cells (rMSCs). rMSCs was characterized by flow cytometry analyses using specific cell surface markers: anti-rabbit CD 73 Allophycocyanin (APC), CD 90 Fluorescein isothiocyanate (FITC) for positive markers, CD 34 phycoerythrin (PE), CD 45 phycoerythrin-cyanine 5.5 (PE/Cy5.5) for negative markers of rMSCs. rMSCs (5×10^6 cells) were suspended in PBS and incubated in the dark with the monoclonal antibodies described above during 20 min. To remove excess antibodies, cells were washed with PBS at 2000 g for 5 min. Cells were analyzed with FACS Aria III flow cytometry system (BD, Biosciences) and data were analyzed by FACS Diva 7.0 Software (BD, Biosciences). Positive labelled MSCs were sorted into collecting tube for the following culture.

Differentiation capacity of rabbit mesenchymal stem cells (rMSCs). *For chondrogenic differentiation;* rMSCs (1×10^4 cells) were cultured in 6 well plates in the chondrogenic medium which was DMEM consist of 10% FBS, 1% penicillin/streptomycin/amphotericin B, 100 μM dexamethasone, 10 ng/ml TGFβ, 10 ng/l IGF, 50 μg/ml ascorbic acid and 50 mg/ml ITS+Premiks at 37°C, 5% CO_2 and 95% humidity. The culture medium was replaced every 2 days in the week. After 2 weeks cells were stained with Alcian blue for the observation of proteoglycans produced by chondrogenic cells.

For adipogenic differentiation; rMSCs (1×10^4 cells) were cultured in 6 well plates with the adipogenic medium which was MEM with 10% FBS, 0.5 mM isobutyl-metylxantine, 10 mM dexamethasone, 10 μg/ml insulin, 200 μM indomethacin, 1% penicillin/streptomycin/amphotericin B. The culture medium was replaced every 2 days in the week. After 4 weeks, cells were stained with oil red o to show the presence of intracellular fat droplets indicated adipogenic differentiation.

For osteogenic differentiation; rMSCs (1×10^4 cells) were cultured in 6 well plates with the osteogenic medium which was MEM consist of 10% FBS, 100 nM dexamethasone, 0.05 μM ascorbic acid, 10 mM β-glycerophosphate, 1% penicillin/streptomycin/amphotericin B for 4 weeks at 37°C and 5% CO_2. The culture medium was replaced every 2 days in the week. Osteogenic differentiation was observed by staining with Alizarin red to demonstrate extracellular calcification.

For fibroblastic differentiation; rMSCs (1×10^4 cells) were cultured in 6 well plates with the fibroblastic medium which was α-MEM supplemented with 10% FBS, 1 ng/ml bFGF and 1% penicillin/streptomycin/amphotericin B. On the third day of culture, 5 ng/ml of TGF-β was added to the medium, and the culture was continued for 2 weeks at 37° C and 5% CO_2. The culture medium was replaced every 2 days in the week. Cells were stained with HE to determine the fibroblastic differentiation.

Preparation of meniscus cell population. The cell cocktail was prepared with equal amounts of differentiated chondrocytes, fibroblasts and undifferentiated rMSCs were cultured at the same culture dishes in the cocktail media. As cocktail media, DMEM-HG was used containing 10% FBS, 1% penicillin/streptomycin/amphotericin B, 1 ng/ml bFGF, 10 ng/ml TGF-β, 10 ng/l IGF, 50 μg/ml ascorbic acid, 50 mg/ml ITS+Premiks. 1×10^5 cells of each cell type were seeded in 6 well plates and cultured at 37°C, 5% CO_2, and 95% humidity for 14 days. Differentiated chondrocytes, fibroblasts, and undifferentiated rMSCs were cultured with chondrogenic and fibroblastic and cocktail medium respectively and used as control groups. Cell proliferation were analyzed on 3, 7, and 14 days of culture period. In addition, number of the three different cells in same culture dish were quantified by Image J software. For 3 samples, 10 fields of view in the culture dish were imaged at 10x magnification. Each image was converted into an 8-bit grayscale image and the cell number was quantified using the

threshold tool. Results are presented as mean ± standard deviation.

Recellularization of decellularized meniscus tissue. Whole decellularized meniscus tissues were cultured with meniscal cells that obtained from rMSCs. Three groups were used for recellularization study; (i) chondrocyte (ii) fibroblast, and (iii) cocktail cells consist of fibroblasts, chondrocytes and fibrochondrocytes. Decellularized meniscus scaffolds were placed in 24 well plates then 1×10^6 cells/ml (for each group) were injected into decellularized tissue (10x5x2 mm^3) to provide cell infusion. Cell seeding was performed with 2 injections of 20 µl of culture medium using 25-gauge insulin syringe for each zone (red, red-white, white). All injections have been performed carefully from the top side of the zones and the cells injected into the middle sections of the tissue. After the injection, tissues were incubated at 37°C, 5% CO_2 atmosphere for 1 hour to allow the cell adhesion. Then 2 mL chondrogenic, fibroblastic, and cocktail medium mentioned above were added on each scaffold in chondrocytes, fibroblasts, and cocktail cells groups respectively. The culture medium was half changed every 2 days in a week. Cell proliferation and cytotoxicity of the recellularized meniscus scaffold were carried out during 14 days of culture period.

Cell proliferation assay. Proliferation of the cells on recellularized meniscus scaffold was determined by XTT cell viability assay during 14 day of culture period. XTT (2,3-bis-(2-methoxy-4-nitro-5-sulfophenyl)-2H-tetrazolium-5-carboxanilide) solution were prepared according to the manufacture's protocol and added until the meniscus scaffolds (n = 3 for each group) covered (500 um) then incubated for 4 h at 37°C. The principle of this method depends the measurement of highly colored formazan dye by dehydrogenase enzymes in metabolically active cells. Therefore, the amount of the formazan produced is proportional to viable cells in the sample. At the end of the incubation time the medium content was transfer to 96-well plates and the absorbance of the formazan was measured colorimetrically by spectrophotometer (Sinergy HTX) at 450 nm wavelength. All experiments were performed in triplicates.

Toxicity assay. Toxicity analysis of recellularized scaffolds (n = 3 for each group) were performed on days 3, 7 and 14 during the cell culture period based on the lactate dehydrogenase (LDH) activity. First, the cell lysis solution in the kit was added to the medium and incubated at 37°C for 45 minutes. Then, the medium content was transfer to 96-well plates, the reaction mixture was added and incubated for 30 minutes. At the end of the incubation, the amount of LDH released into the medium was measured colorimetrically with a spectrophotometer (Sinergy HTX) at 490–680 nm wavelength. All experiments were performed in triplicates.

Histology. Recellularized meniscus scaffolds were stained with HE, Ab, and Mt to observe the cellular distribution, collagen arrangement, and GAG structure. All samples were evaluated considering red, white- red, and white zone. Subsequently, stained samples were analyzed by the histological scoring system to determine the cellular density according to all zones. ImageJ software was used to quantify the number of cells in HE stained recellularized meniscus sections. For each sample, 5 fields of view throughout the recellularized meniscus section were imaged at 20x magnification (total of 15 fields per meniscus). Each image was converted to a grayscale (8-bit) image in ImageJ, and the number of cells was quantified using the threshold tool. Results from each group (n = 3 meniscus per fibroblast, chondrocytes, fibrochondrocytes groups) were presented as mean ± standard deviation.

In addition to the histological stainings recellularized meniscus tissues were evaluated in terms of DNA, GAG and collagen contents. Biochemical assays were performed in triplicates.

Statistics. All values are reported as mean ± standard deviation. Student's t-test or one-way analysis of variance (ANOVA) were performed to compare native and decellularized meniscus tissue specimens. A significance level of 95% with a $p < 0.05$ considered statistically significant.

Results

Verification of decellularization process

Histology. After the decellularization process meniscus tissues were stained with HE for general morphology, Mt for collagen fibers, Ab for GAG structure. In native meniscus, meniscal cells were observed to be intense toward the vascularized red zone (Figure 2 (a1)) but also in red-white (Figure 2 (a2)) and white zone (Figure 2(a3)). Besides, radial and circumferentially orientated collagen fibrils were visualized with Mt staining in all zones (Figure 2 (c1, c2, c3, c4)) and GAG concentration was found to be dense around the red, red-white, white and superficial zones as shown in Ab staining (Figure 2 (e1, e2, e3, e4)).

After the decellularization process, cellular content of the meniscus tissues was removed, and it was shown that absence of cells in lacunae (Figure 2 (b1, b2, b3, b4)) when compared with the native tissues. In addition to the HE staining, ECM components of meniscus were observed with MT and Ab. Collagen fibrils, cytoplasm

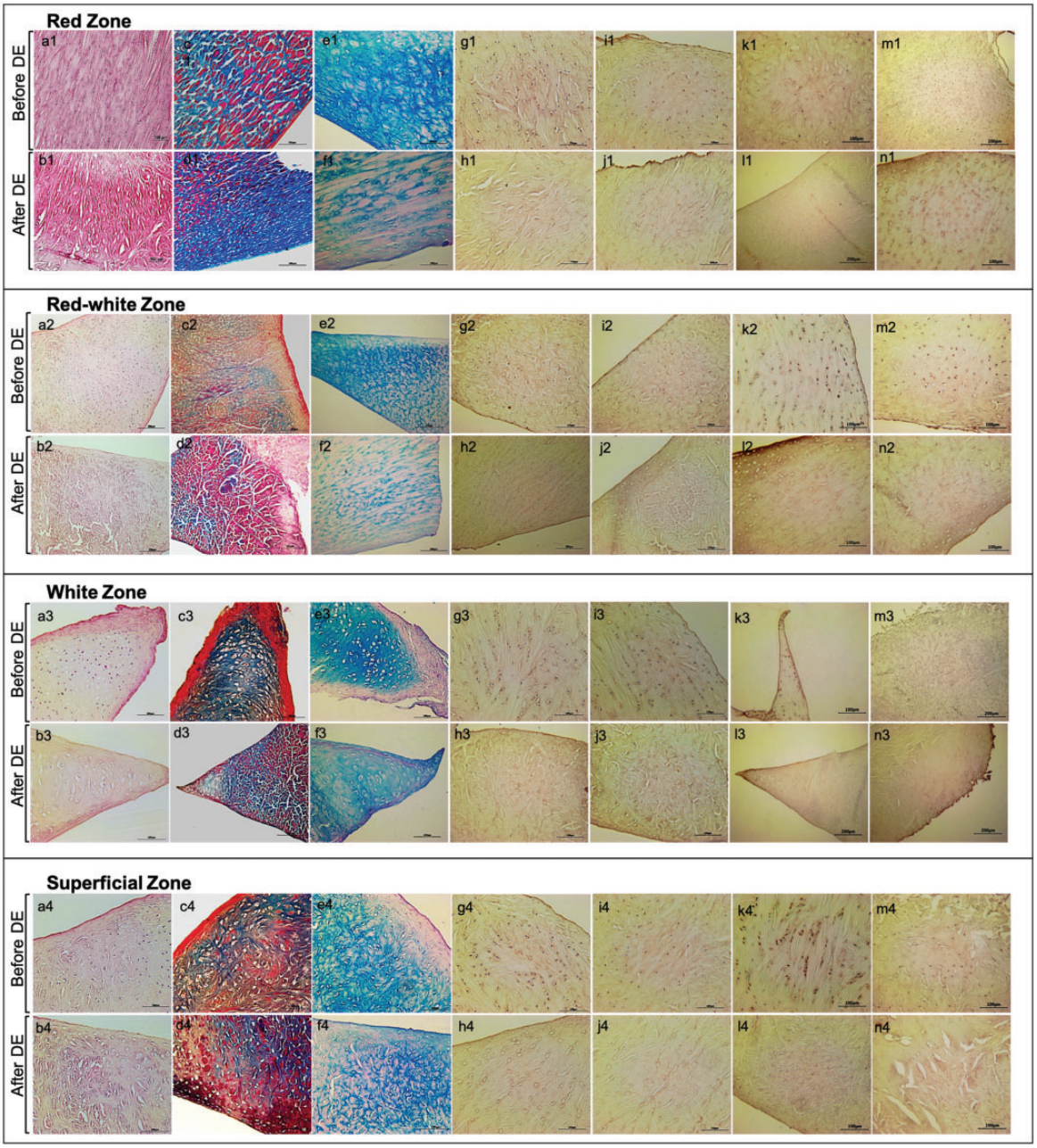

Figure 2. Red, red-white, white and superficial zones of meniscus tissues stained with HE (a1-4, b1-4), Mt (c1-4, d1-4), Ab (e1-4, f1-4), collagen type I (g1-4, h1-4) and type II (i1-4, j1-4), aggrecan, (k1-4, l1-4) and vimentin (m1-4, n1-4) before and after decellularization process. DE: decellularization.

and nucleus were stained blue, red/pink and dark blue respectively in Mt staining (Figure 2 (c, d)). Images revealed that collagen structures were maintained in decellularized meniscus tissues and were observed with radial direction around the empty lacuna (Figure 2(d1, d2, d3, d4)). Ab staining showed that GAG structures as bright blue both native meniscus tissue (Figure 2 (e1, e2, e3, e4)), and decellularized meniscus (Figure 2 (f1, f2, f3, f4)).

Collagen type I, type II, aggrecan and vimentin structures in native and decellularized meniscus were evaluated immunologically. Distribution of the collagen type I was shown to be present in the native meniscus in all zones and positive staining was seen around cells especially red and red-white zones (Figure 2(g1, g2, g3, g4)). The intensity of the staining appeared to remain unchanged after decellularization with absence of cells (Figure 2 (h1, h2, h3, h4)). Collagen II was seen

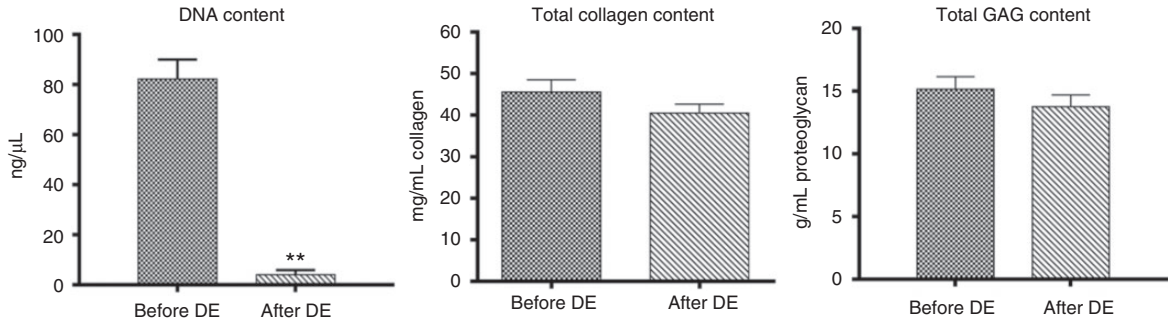

Figure 3. Total DNA, collagen and GAG content of native and decellularized meniscus tissues. All experiments were performed in triplicates. (Avr±SD, $^{**}p < 0.05$) DE: decellularization.

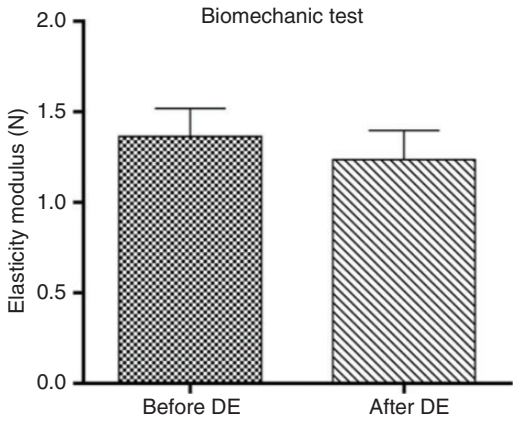

Figure 4. Elasticity modulus of native and decellularized meniscus tissue. DE: decellularization.

in the native meniscus in all zones especially around cells localized in the red zone (Figure 2 (i1)), white zone (Figure 2 (i3)) and superficial zone (Figure 2 (i4)), also staining intensity remained unchanged after decellularization (Figure 2(j1, j2, j3, j4)). Aggrecan stained more intensely outer parts in red-white zone and white zone both native (Figure 2 (k2, k3)) and decellularized tissue (Figure 2 (l2, l3)). Vimentin stained predominantly around the lacunae of the cells in native and decellularized tissue, it was seen that the presence of vimentin around the lacunae of the entire decellularized tissue (Figure 2 (n1, n2, n3, n4)).

Histology and immunohistochemistry results clearly showed that the decellularization process did not affected to the histoarchitecture of the tissue.

Biochemical analysis. Total DNA, collagen and GAG content of both native and decellularized meniscus tissues were determined quantitatively (Figure 3). Total DNA content of native meniscus was 80.5 ng/mg and decellularized meniscus was 5.02 ng/mg. There are significant differences between two groups ($p < 0.05$). The collagen content of the native and decellularized meniscus tissue were determined as $46{,}63 \pm 0.41$ ug/mg, $43{,}40 \pm 0.80$ ug/mg respectively. The total GAG content of native tissue was 14.95 ± 0.60 ug/mg and for decellularized tissue was 13.03 ± 0.37 ug/mg. There were no significant differences in collagen and GAG content according to statistical analysis (student's t-test; $p > 0.05$). Biochemical measurements gave quantitative evidence of the decellularization process did not affect the histoarchitecture of the meniscus tissue with removing cell content in the tissue.

Biomechanic test. Native and decellularized meniscus ($n = 6$) were tested under compression to determination of compressive strength. There was no significant difference between elasticity modulus of native meniscus tissue which was 1.365 N and decellularized meniscus tissue which was 1.236 N (Figure 4). In concluded that decellularization process did not affect the biomechanical properties of meniscus tissue.

In vitro cell culture studies

rMSCs were isolated from rabbit bone marrow then cultured for 14 days. Figure 5A represented that spindle-shaped and elongated fibroblast-like cells at P1, P2, P3. Cells demonstrated increased proliferation and uniformly maintaining a homogeneous fibroblastic morphology.

The cultured rMSCs ($5x10^6$ cells) were analyzed the expression of positive and negative surface markers by flow cytometry for identification. CD 90 and CD 73 were used as positive surface markers and CD 45 and CD 34 were used as negative surface markers which are labeled with FITC, APC, PE/Cy5.5, and PE respectively. Results revealed that cells were positive for CD 90 and CD 73 and were negative for CD 45 and CD 34 as expected. It was found that 0.3% of cells (P2) and 0.1% of cells (P5) expressed negatively rMSCs markers (CD 34 and CD 45) and 98.1% of cells (P3) and 98.7% (P4) expressed positively rMSC markers (CD 73 and CD 90), thereby demonstrating a characteristic

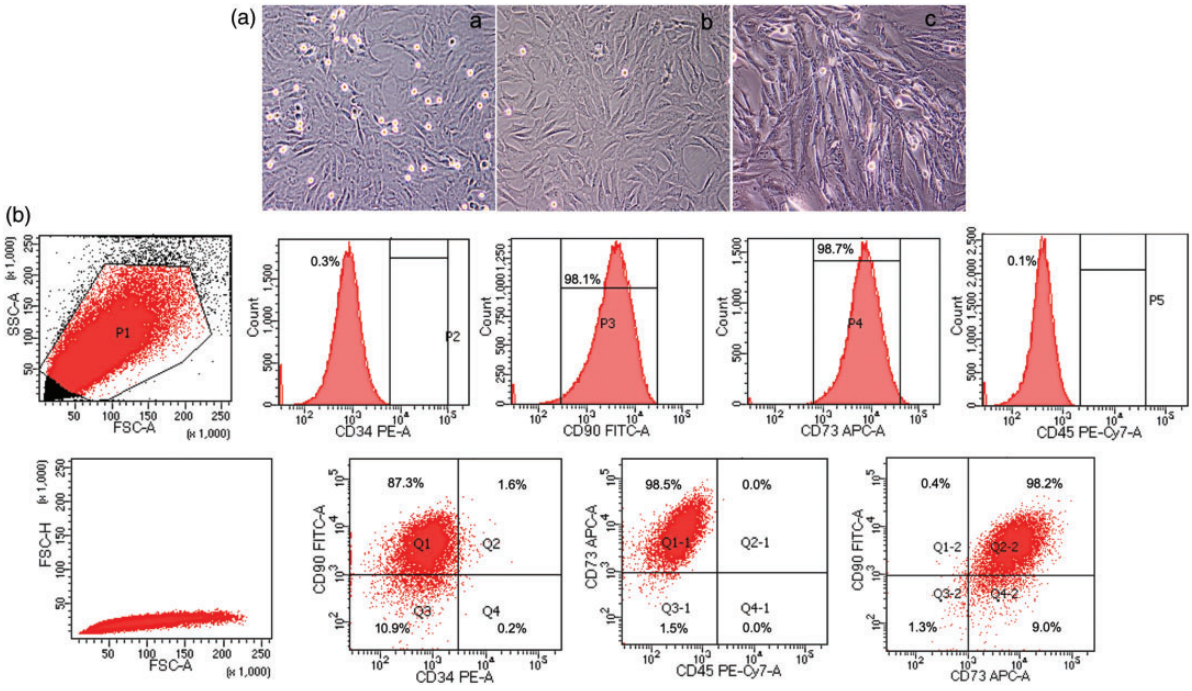

Figure 5. A. Microscopic images of the rMSCs at P1(a), P2(b), P3(c). B. Flow cytometric cell characterization and cell sorting. Flow cytometric validation of rMSCs with CD 34, CD90, CD 73, CD 45 and details from sorting demonstrating the overall cell distribution of negative for CD 34 and CD 45 and positive for CD 73 and CD 90.

immunophenotype of rMSC. In addition, quadrants were set to delineate the negative and positive populations and quadrant regions showing the percentage of cells in each sub-population. 98.2% (Q2-2) double-positive cells for CD 90 and CD 73 shown in dot plots image were sorted for recellularization study (Figure 5(B)).

Differentiation capacity of rabbit mesenchymal stem cells (rMSCs). Differentiation capacity of rMSCs were evaluated by histological staining. During chondrogenic differentiation, cells appeared round shape and secreted proteoglycans by differentiated chondrocytes were observed in blue color with alcian blue staining (Figure 6 (a) and (e)). At the end of the 2 weeks of the culture period, spindle-shaped fibroblast cells were observed in fibroblastic media (Figure 6 (b) and (f)). In osteogenic differentiation, mineralization sites of the ECM were observed with alizarin red staining (Figure 6 (c) and (g)). Also, oil droplets which are the characteristic of adipogenic differentiation were observed in red with oil red o staining (Figure 6 (d) and (h)).

Preparation of meniscus cell population. To prepare meniscus cell population a cocktail of the cells which consist of differentiated chondrocytes, differentiated fibroblasts and non-differentiated MSCs were seeded in the same wells. The specific cell population of the meniscus tissue was observed after 14 days of the culture period by microscopically. Microscopic investigations revealed spindle-shaped cells like fibroblasts, round shape cells like chondrocytes and multicytoplasmic forms like fibrochondrocytes are being in the cocktail of the cell preparation (Figure 7 (a) and (b)). In addition, Figure 7 (c) is represented that cell number of three different cells in the same culture plate. Distribution of the cells was quantified that 85%, 62%, and 54% for fibrochondrocytes, chondrocytes, and fibroblasts.

Proliferation capability of the cocktail cells was examined by XTT cell proliferation assay also. The analyses were performed on 3, 7 and 14 days of the culture period. The results indicated that cell proliferation increased for 14 days and statistically significant differences were found of the cocktail cells compared to the fibroblast, chondrocyte and MSCs groups ($p < 0.05$) (Figure 8).

Recellularization of the decellularized meniscus tissues

Cell proliferation. Proliferation capacity of the fibroblast, chondrocytes and cocktail cells in decellularized meniscus were evaluated by XTT cell viability assay. It was found that cells were proliferated in decellularized tissues with increasing trend in all groups for 14 days (Figure 9). Cocktail cells showed highest proliferation

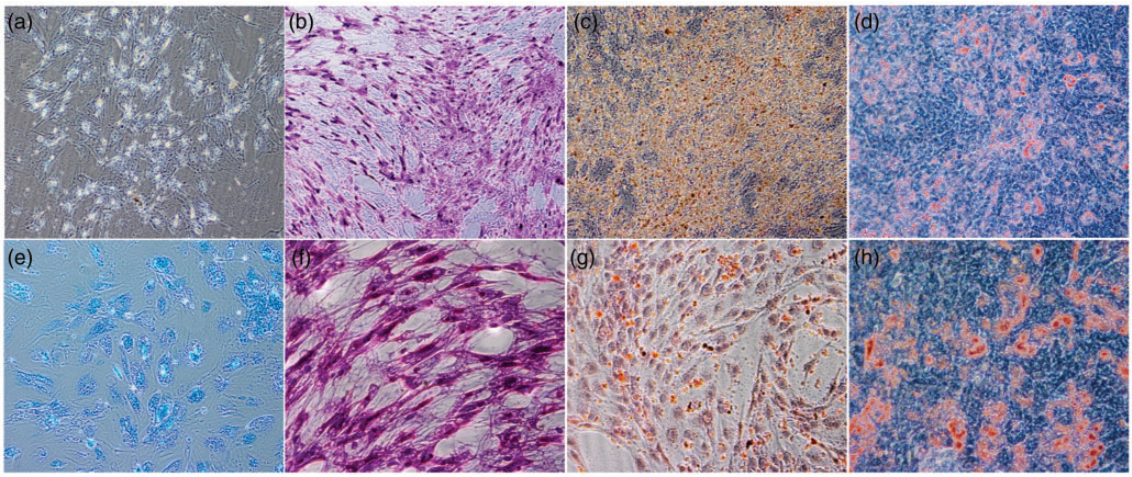

Figure 6. Chondroctye (a,e), fibroblast (b,f), osteoblast (c,g) and adipocyte (d,h) differentiation of rMSCs. Magnifications a-b-c-d 10X, e-f-g-h 20X.

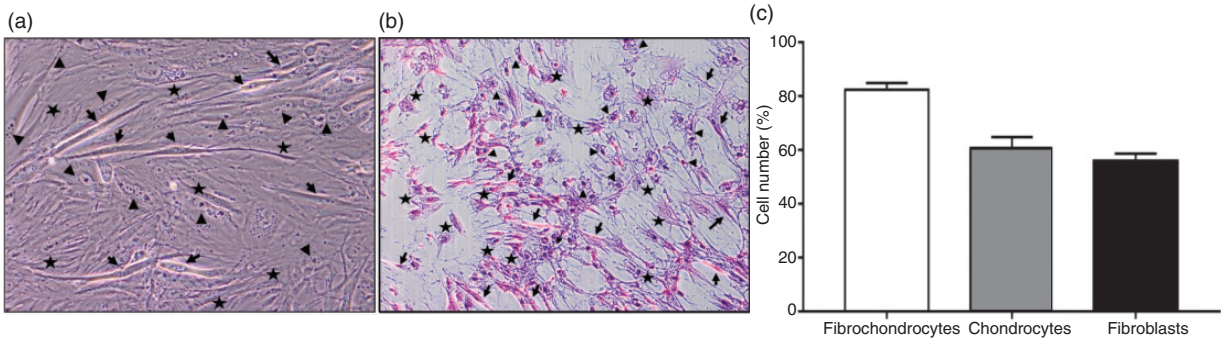

Figure 7. Inverted microscopy images (a) and Hematoxylin eosin staining images (b) of cocktail cells after 14 days of incubation period. Spindle-shaped fibroblast (arrows), round-shaped chondrocytes (triangles), fibrochondrocytes with multiple projections (stars) were shown in the same culture plate (Magnification 20X). Cell number (%) of fibrochondrocytes, chondrocytes, and fibroblasts in the cocktail cells (c).

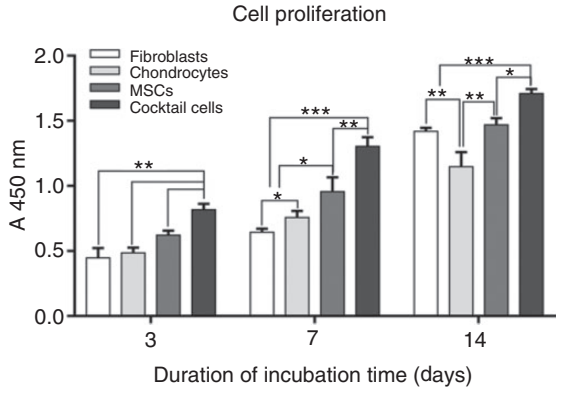

Figure 8. Cell proliferation test results of fibroblasts, chondrocytes, MSCs and cocktail cells. All experiments were performed in triplicates. (*$p < 0.5$, **$p < 0.01$, ***$p < 0.001$).

capacity, and there were statistically significant differences in the cocktail cells group compared to the fibroblast and chondrocyte groups.

Cytotoxicity. Cytotoxic effects of decellularized meniscus on the fibroblasts, chondrocytes and cocktail cells were evaluated by LDH assay. Decellularized meniscus did not show any cytotoxic effect on cells during incubation time. The results showed similarity and did not statistically significant differences in all groups for 14 days of incubation (Figure 9).

Histological evaluation of recellularized meniscus tissue. Recellularized whole meniscus tissues were evaluated by histological staining in terms of cells-tissue interaction and localization of cells in the lacuna of decellularized tissues. Recellularized meniscus with fibroblasts, chondrocytes and cocktail cells were

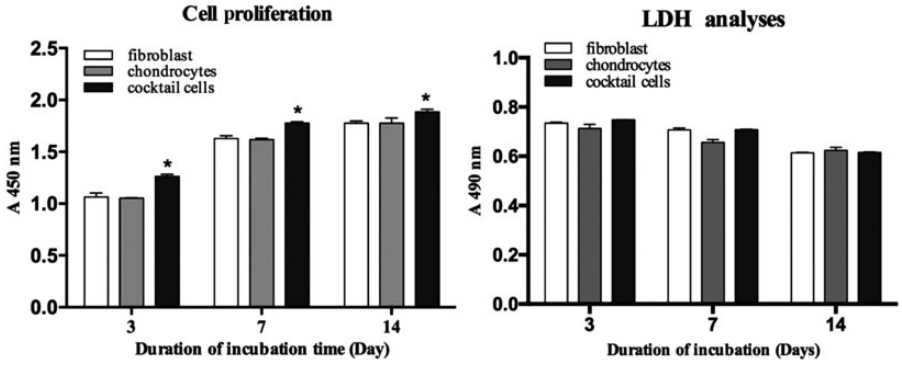

Figure 9. Cell proliferation and cytotoxicity analyses of cells on the recellularized tissues. (*$p < 0.05$) All experiments were performed in triplicates.

evaluated as red, red-white and white zone by HE, MT and Ab staining (Figure 10).

In fibroblast seeded culture, cells were mainly localized in red (Figure 10 (a1)) and red-white (Figure 10 (b1)) zone compared to the white zone of the tissue Figure 10 (c1). Circumferential collagen structures of the recellularized tissue were shown by MT staining in all zones (Figure 10 (d1), (e1), (f1)). In addition, Ab staining represented that fibroblasts secreted more amounts of GAG (shown as dark blue) in the white zone (Figure 10 (i1)). Light colored Ab staining indicated a smaller number of cells in the inner zone of tissue (Figure 10 (h1)).

In chondrocyte seeded culture, cells were observed mainly red-white (Figure 10 (b2) and white (Figure 10 (c2)) zone of the tissue after 14 days culture. Collagen fibers which were stained with MT were seen dark blue or dense in all zones (Figure 10 (d2), (e2), (f2)). Ab staining indicated that GAGs were secreted by chondrocytes in red-white (Figure 10 (h2)) and white (Figure 10 (i2)). zones. In the red-zone, chondrocytes secreted more amount of cytoplasm as seen in pink color compared to the other groups (Figure 10 (g2)).

In cocktail cells seeded culture, cells were broadly distributed in all zones and localized in empty lacunas of the decellularized meniscus tissue (Figure 10 (a3), (b3), (c3)). MT stainings demonstrated that cocktail cells were well arranged between collagen fibers and fibers orientation were seen as dark blue in the red (Figure 10 (d3)), red-white (Figure 10 (e3)) and white zones for 14 days (Figure 10 (f3)). In addition, Ab staining showed that more amounts of GAG secreted by cocktail cells were observed as dark blue in all zones of the tissue (Figure 10 (g3), (h3), (i3)).

Histological results indicated that fibroblasts, chondrocytes, and cocktail cells proliferated and localized in the lacuna of the decellularized meniscus tissues, but cocktail cells were more proliferated and well distributed than chondrocytes and fibroblasts.

Histological scoring. In addition to the histological staining, cellular distribution and number of cells in each zone of the recellularized meniscus scaffolds were evaluated by Image J Software. The results represent that 170.8 ± 14 fibroblasts, 159.8 ± 10 chondrocytes, 230.3 ± 12 cocktail cells were found in red zone, 149 ± 8 fibroblasts, 176.8 ± 6 chondrocytes, 216 ± 9 cocktail cells were found in red-white zone, 110 ± 9 fibroblasts, 204.4 ± 4 chondrocytes, 202.4 ± 6 cocktail cells were found in white zone in recellularized meniscus scaffolds (Figure 10). There is statistically significant difference for number of cocktail cells compared to the fibroblasts and chondrocytes groups.

Biochemical contents of recellularized meniscus. DNA, collagen and GAG contents of recellularized meniscus tissues were evaluated after 14 day of culture period by biochemical analysis (Figure 11). DNA contents of recellularized tissues were found in 62.267 ± 1.84 ng/µl, 66.662 ± 3.29 ng/µl, 77.492 ± 3.02 ng/µl for fibroblast, chondrocytes and cocktail groups respectively. Total collagen contents were determined 73.008 ± 3.08 mg/ml, 89.709 ± 1.31 mg/ml, 116.769 ± 5.74 mg/ml for fibroblast, chondrocytes and cocktail groups respectively. Total GAG contents were estimated in fibroblast culture 14.485 ± 0.60g/ml, in chondrocytes culture 17.476 ± 0.71g/ml, in cocktail culture 18.928 ± 0.36g/ml. In all biochemical tests, there are statistical differences in cocktail cells compared to both fibroblasts and chondrocytes groups ($p < 0.05$).

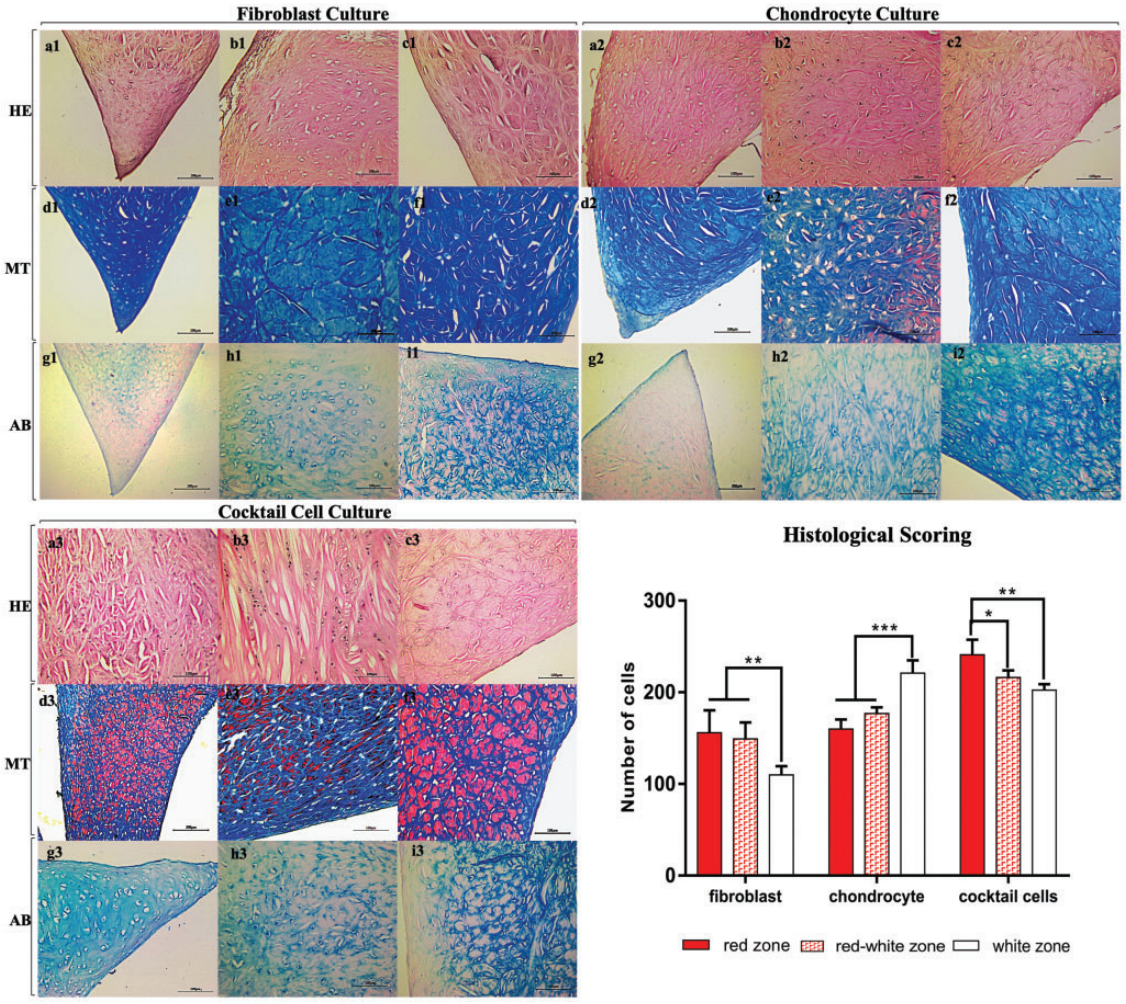

Figure 10. Histological images and quantification results of recellularized meniscus tissues with fibroblasts, chondrocytes, and cocktail cells on the red (a1-3, d1-3, g1-3), red-white (b1-3, e1-3, h1-3) and white zones (c1-3, f1-3, i1-3).

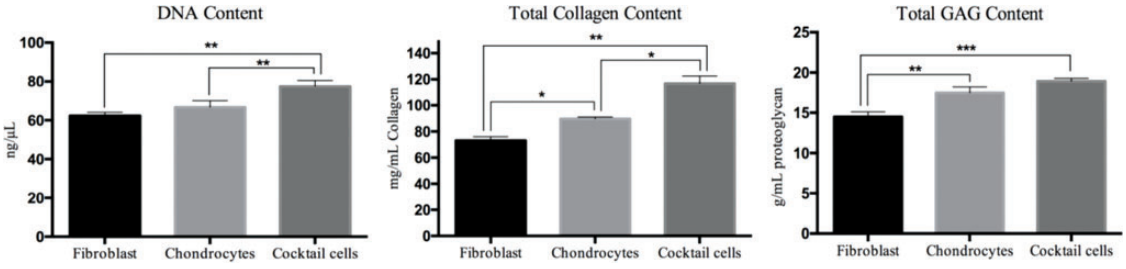

Figure 11. Total DNA, collagen and GAG content of the recellularized meniscus tissue. (*$p < 0.05$, **$p < 0.01$, ***$p < 0.001$) All experiments were performed in triplicates.

Discussions

The meniscus tissue has poor healing potential, due to the partly absence of vasculature. The lesions occurred in the avascular zone show no or limited tendency to heal and it should be resected by partial or total meniscectomy.[27–29] Tissue engineering and regenerative medicine research offer significant approaches to develop advanced materials that can better mimic the architecture and functional properties of native tissues. Recently, natural and synthetic scaffolds have been reported with plenty of studies as a possible biomaterial for meniscal regeneration.[30–33] Moreover, collagen meniscus implants,[5,31,34,35] polyurethane meniscus implants,[36,37] silk fibrous protein scaffolds,[33,38,39]

polycaprolactone scaffolds[40–42] and polyester–carbon cell-free implants[43] have been used to mimic the meniscus tissue. However, these biomaterials have different characteristic features comparison to natural menisci in terms of different organization and interactions among the major components (water, GAGs and collagen) of the meniscus. The optimal biomaterials for meniscus replacement still need to be developed due to the meniscus has distinctive three-dimensional structure and unique biological characteristics as well as biomechanical properties. Therefore, decellularized ECM scaffolds are extensively investigated as a natural substitute for regeneration of tissue.

Tissues treated with different solutions to remove cellular component can provide an optimum decellularized biological scaffold material for meniscus tissue engineering. However, the removal of cells during this process ECM can be damaged. Although, different decellularization methods have been reported in the literature, to find an effective and least destructive method are still required. Decellularization of the meniscus is much more difficult since it is composed of fibrocartilage and collagen with a tightly packed ECM structure.[44] Different detergent combinations which are sodium dodecyl sulfate (SDS, an ionic detergent), Triton-X (a non-ionic detergent) and tri-nitrobutyl phosphate (TnBP) have been used for meniscus decellularization.[9,34,45,46] Currently, a variety of decellularization and recellularization methods used in meniscus tissue engineering have been reported in the literature but there is no consensus on the optimal procedure to generate decellularized meniscus or their application.

Maier et al. decellularized ovine meniscus using enzymatic solution included trypsin, collagenase, protease and removed meniscal cells and major histocompatibility complex molecules. Although researchers claimed that biomechanical properties remained the same, GAG contents were decreased compared to the native tissue due to the harmful effects of enzymatic treatment.[47] According to the studies, it is seen that only enzymatic treatment is not adequate. Therefore, we agreed with the literature that suggest the conjunction of physical and chemical methods.[21,48,49] Detergents such as SDS and Triton X-100 are generally used to remove cellular components of the tissues. But the efficacy of the detergents and the damage levels of the tissue are important points. Although Sandmann et al.[46] reported that decellularized human meniscus with 2% SDS without compromising biomechanical properties, research revealed that SDS can cause collagen damage such as fragmentation and swelling of the fibers.[50] Therefore, we conclude that the combination of the physical, chemical and enzymatic methods and incubation periods of the detergents are important for the decellularization procedure.

In this study, the combination of physical, chemical and enzymatic methods was used for meniscus decellularization based on modifications of Stapleton et al.'s method.[21] Tissue samples were investigated histologically considering red, red-white, white and superficial zones and our results showed that cellular components of the meniscus were removed from all zones within 14 days of decellularization process (Figure 2 (b1), (b2), (b3), (b4)). In addition, biochemical tests showed that the DNA content were significantly decreased after decellularization (Figure 3) which are confirmed by histological results. Mt staining results revealed that collagen fibers were maintained in decellularized meniscus tissues (Figure 2 (d1), (d2), (d3), (d4)) which provide information that our method has no harmful effect on ECM of the meniscus tissue. In addition, biochemical assay results supported the histological staining quantitatively (Figure 3). In the Stapleton method, GAG content, which is one of the main structures of the ECM, was decreased by 59.4% after the decellularization process.[21] Although our method is based on the Stapleton method, we did not find statistically significant differences ($p > 0.05$) in collagen and GAG content between before and after decellularization. GAG structures were also observed in bright blue color after decellularization in histological staining (Figure 2 (f1), (f2), (f3), (f4)) which was supported by the biochemical analysis results (Figure 3). Therefore, we conclude that our decellularization method and modifications are more effective for the protection of GAG and ECM structure.

The biomechanical feature of the meniscus tissue is important due to its tensile and shock absorption properties.[29,51–53] Another important outcome of the optimum decellularization method is the removal of cells from the tissue without affecting biomechanical properties. Various physical and enzymatic methods such as repeated freezing/thawing, high-pressure treatments, gamma irradiation, and enzymatic treatment with collagenase, trypsin were used for decellularization of the tissues.[44,54,55] However, it was reported that only physical or enzymatical treatments were adversely affected the biomechanical features of the meniscus. Combination of different decellularization methods provides the minimum degeneration of tissue architecture. In our combinational decellularization method, the biomechanical features of the meniscus tissue did not change. There is no statistically significant difference in biomechanical properties before and after decellularization. Our results gave evidence of the separation of cellular content in all locations with the preservation of the main histoarchitecture and biomechanical properties following the decellularization process.

The other advantage of our decellularization method is short incubation time and without the use of expensive and generally preferred chemical aprotinin as a protease inhibitor to prevent ECM damages during decellularization applications.[56] Although aprotinin has been generally suggested for the decellularization method, we successfully performed decellularization process with only SDS detergent which also provides cost effectivity.

The approach of recellularization of the decellularized tissues arise from the clinical usage of decellularized matrices and decellularized organs.[57–60] In tissue engineering, several types of cells such as fibroblasts, chondrocytes or isolated cells from meniscus used to repopulate tissue-specific ECM scaffolds to eventual functionality and clinical success of engineered constructs.[33,61–63] Additionally, fibrochondrocytes, obtained from meniscus, are the most common preferred cells in the meniscus regeneration, however their proliferative capacity in human decreases with age.[24,64] MSCs are known to have an ability to differentiate into cells of the mesenchymal lineage and a capacity for self-renewal and may be a good choice for meniscus regeneration.[26,65] Mandal et al. produced silk scaffold and seeded with human MSCs to mimic meniscus tissue, significant upregulation of cartilage related ECM markers were found.[33] Another study reported that meniscal cells cultured with MSCs showed higher expression of collagen and GAG, which is induced meniscal phenotype.[66]

On the basis of these studies, in our study, the meniscus cell population (cocktail cells) consists of fibroblasts, chondrocytes and fibrochondrocytes obtained from differentiated rMSCs. In our proliferation results, both fibroblasts and chondrocytes were shown high proliferation levels with increasing trend, but the cocktail cells showed more proliferative capacity during the 14 days of the culture period. Cell number (%) of fibroblasts, chondrocytes, and fibrochondrocytes in the same culture plate were also quantified by Image J software. The results showed that three cell types proliferated in more than 50% ratio in the culture plate. However, cocktail cells proliferated by 85% on the same plate, and this ratio was found to higher than fibroblasts (62%) and chondrocytes (54%). According to cell culture results, we conclude that incubation of fibroblasts, chondrocytes, fibrochondrocytes, and MSCs in the same environment might provide appropriate niche and cytokine secretion to increase the proliferation capacity of the cells.

The immunological response of the scaffold materials should be evaluated in more detail with in vivo studies however, cytotoxic effect, cell proliferation, and distribution on the decellularized scaffolds can provide an idea for in vitro level. The predictive plasticity and macrophage polarization on the decellularized scaffold surface help gain detailed information regarding the immunological response.[67,68] However, cell-mediated cytotoxicity plays an important role in the host immune defense.[69] The proliferation and cytotoxic assays are widely used for the biological potential determination of biomaterials. Also, these procedures are widespread applications for many vaccines, diagnosis of infectious disease, and drug discoveries before in vivo experiments.[70,71] In this study, cytotoxicity, cell proliferation, and distribution in the decellularized meniscus tissue were determined to assess the biological compatibility of the decellularized scaffolds. Besides the continuous proliferation trend of cells on the decellularized scaffolds and no cytotoxic effect, preserved ECM architecture has helped the regulation of the cellular distribution and proliferation.

Cell attachment and proliferation in the decellularized tissues are part of the remodeling process wherein cells begin to infiltrate and secrete growth factors after adhesion.[72] Moreover, MSCs have high proliferation capacity and secrete many trophic and bioactive factors as well as synthesize stimulatory ECM components.[73] According to our histological results after recellularization, cocktail cells were localized in the empty lacuna in all zones of the decellularized tissue and showed more proliferation capacity. It may result from the fact that MSCs have more proliferation capacity and that cocktail cells are more suitable cell populations for meniscus tissue.[73] The consistency with the 2 D cell culture results, cocktail cells showed more proliferation capacity in recellularized meniscus scaffolds as well as higher DNA content. Increasing the DNA level indicated that the cells, especially cocktail cells, proliferated in recellularized meniscus during the culture period. Moreover, Image J analysis results have also represented distribution of the number of cells according to the zones (Figure 10). While fibroblasts are distributed in the red zone of the meniscus scaffold, chondrocytes were mostly localized in the red-white and white zone. Besides, cocktail cells were most proliferated in the red zone of the meniscus scaffold, but they were also localized in the red-white and white zones. In addition, the increase in the number of cocktail cells from the white zone to the red zone showed the similarity in natural meniscal cell distribution[66,72] and recellularized meniscus scaffolds have the potential to mimic the meniscus tissue in terms of cellular population.

The primary compositions of the ECM such as collagen, proteoglycans and GAG have generally been used as a criteria for the identification and evaluation of the chondrogenic capacity of the cells or constructs.[74] The highest amount of collagen and GAG levels were obtained from the recellularization group seeded with cocktail cells (Figure 11). It may result from by the presence of chondrocytes and fibrochondrocytes in the cocktail cells, also leads to the highest amount collagen and

GAG levels. The results also revealed that decellularized meniscus has potential for promoting cell proliferation and provides a natural substrate to production of ECM proteins like collagen or GAG with cocktail cells. In our best knowledge, recellularization of the decellularized meniscus using cocktail cells obtained from both differentiated and undifferentiated rMSCs has not yet been investigated. This is the first study that designed an in vitro co-culture system for obtaining meniscal cell population with the basic cellular morphology of rabbit meniscus has been identified. In this study we revealed that our recellularization and decellularization methods provide a biomaterial that mimics native meniscus tissue as ultrastructural characteristics and the biochemical compositions.

Conclusion

In this study, we demonstrated a modified decellularization and recellularization methods for meniscus tissue by removing cellular components and preserving the ECM without any significant loss in mechanical properties. The significant outcomes of the study are decellularization of meniscus tissue with minimum percentage of detergent in a short incubation time and recellularization of meniscus tissue with cocktail cells mimicking native meniscus cell population. The promising results may be attributed to the decellularized meniscus scaffold, which provided an appropriate microenvironment to avoid any adverse immune response by allogeneic or xenogeneic recipients of the ECM scaffold material. In addition, this study demonstrates that the meniscal cell population could be obtained using MSCs and recellularized meniscus could be efficient to develop functional decellularized meniscus for clinical applications. In future in vivo studies, we anticipate showing that the recellularized meniscus scaffold will support the appropriate microenvironment to promote cell growth and appropriate host response.

Acknowledgements

The authors are grateful to Izmir Biomedicine and Genome Center (IBG) for flow cytometry analysis.

Declaration of conflicting interests

The author(s) declared no potential conflicts of interest with respect to the research, authorship, and/or publication of this article.

Funding

The author(s) disclosed receipt of the following financial support for the research, authorship, and/or publication of this article: This study was supported by Dokuz Eylul University, Department of Scientific Research Project (2015.KB. SAG.039).

ORCID iD

Semra Koçtürk https://orcid.org/0000-0001-7528-1845

References

1. McDermott ID and Amis AA. The consequences of meniscectomy. *J Bone Joint Surg Br* 2006; 88-B:12: 1549–1556.
2. Markes AR, Hodax JD and Ma CB. Meniscus form and function. *Clin Sports Med* 2020; 39: 1–12.
3. Rao AJ, Erickson BJ, Cvetanovich GL, et al. The meniscus-deficient knee. *Orthop J Sport Med* 2015; 3: n. pag.
4. Rodkey WG, Steadman JR and Li ST. A clinical study of collagen meniscus implants to restore the injured meniscus. In: *Clinical orthopaedics and related research* 1999; 367 Suppl: 281–292.
5. Houck DA, Kraeutler MJ, Belk JW, et al. Similar clinical outcomes following collagen or polyurethane meniscal scaffold implantation: a systematic review. *Knee Surg Sports Traumatol Arthrosc* 2018; 26: 2259–2269.
6. Torres SJ, Hsu JE, Mauck RL. Meniscal Anatomy. In: Kelly JD (eds) *Meniscal Injuries*. 4th ed. New York: Springer 2014, pp.1–7.
7. Verdonk P. Histology-Ultrastructure-Biology. In: Beaufils P, Verdonk R (eds) *The Meniscus*. 2nd ed. Berlin, Heidelberg: Springer, 2010, pp. 19–27.
8. Niu W, Guo W, Han S, et al. Cell-based strategies for meniscus tissue engineering. *Stem Cells Int* 2016; 2016: 4717184.
9. Buma P, Ramrattan NN, Van Tienen TG, et al. Tissue engineering of the meniscus. *Biomaterials* 2004; 25: 1523–1532.
10. Kohn D, Verdonk R, Aagaard H, et al. Meniscal substitutes – animal experience. *Scand J Med Sci Sports* 2007; 9: 141–145.
11. Vårbakken K, Lorås H, Nilsson KG, et al. Relative difference among 27 functional measures in patients with knee osteoarthritis: an exploratory cross-sectional case-control study. *BMC Musculoskelet Disord* 2019; 20: 462.
12. Lohmander LS, Englund PM, Dahl LL, et al. The long-term consequence of anterior cruciate ligament and meniscus injuries: osteoarthritis. *Am J Sports Med* 2007; 35(10): 1756–1769.
13. Kaplan DJ, Glait SA, Ryan WE, et al. Meniscal allograft transplantation made simple: bridge and slot technique. *Arthrosc Tech* 2017; 6(6): 2129–2135.
14. De Bruycker M, Verdonk PCM and Verdonk RC. Meniscal allograft transplantation: a meta-analysis. *Sicot J* 2017; 3: 33.
15. Doral MN, Bilge O, Huri G, Turhan E, Verdonk R. Modern treatment of meniscal tears. *EFORT Open Rev*. 2018; 3(5): 260–268.
16. Badylak SF and Gilbert TW. Extra cellular matrix as a biological scaffold material structure and function. *Acta Biomater* 2009; 5(1): 1–13.
17. Crapo PM, Gilbert TW and Badylak SF. An overview of tissue and whole organ decellularization processes. *Biomaterials* 2011; 32: 3233–3243.

18. Hoshiba T and Yamaoka T. Extracellular matrix scafolds for tissue engineering and biological reseaerch. In: *Decellularized Extracellular Matrix: Characterization, Fabrication and Applications*. Royal Society of Chemistry, 2019, pp. 1–14.
19. Faulk DM, Badylak SF, Natural Biomaterials for Regenerative Medicine Applications, In: Orlando G, Lerut J, Soker S, Stratta RJ (eds) *Regenerative Medicine Applications in Organ Transplantation*, Academic Press, 2014, pp. 101–112.
20. Gupta SK, Mishra NC, Dhasmana A. Decellularization Methods for Scaffold Fabrication. In: Turksen K. (ed) *Decellularized Scaffolds and Organogenesis*. Methods in Molecular Biology, vol 1577. Humana Press, New York, NY, 2017, pp. 1-10.
21. Stapleton TW, Ingram J, Katta J, et al. Development and characterization of an acellular porcine medial meniscus for use in tissue engineering. *Tissue Eng – Part A* 2008; 14 (4): 505–518.
22. Kara A. Development of meniscus tissue bio-compatibility using allograft native scaffold. PhD Thesis, Dokuz Eylul University, TR, 2017.
23. Athanasiou KA, Sanchez-Adams J. Engineering the knee meniscus. In: Athanasiou KA, Kent Leach JK, editors. *Synthesis lectures on tissue engineering*. Williston (VT): Morgan and Claypool Publishers; 2009. p. 1–97.
24. Verdonk PCM, Forsyth RG, Wang J, et al. Characterisation of human knee meniscus cell phenotype. *Osteoarthr Cartil* 2005; 13(7): 548–560.
25. Hayes WC, Keer LM, Herrmann G, et al. A mathematical analysis for indentation tests of articular cartilage. *J Biomech* 1972; 5(5): 541–551.
26. Dominici M, Le Blanc K, Mueller I, et al. Minimal criteria for defining multipotent mesenchymal stromal cells. The international society for cellular therapy position statement. *Cytotherapy* 2006; 8: 315–317.
27. Makris EA, Hadidi P and Athanasiou KA. The knee meniscus: structure-function, pathophysiology, current repair techniques, and prospects for regeneration. *Biomaterials* 2011; 32: 7411–7431.
28. Yagi H, Soto-Gutierrez A and Kitagawa Y. Whole-organ re-engineering: a regenerative medicine approach in digestive surgery for organ replacement. *Surg Today* 2013; 43: 587–594.
29. Verdonk P. Histology-Ultrastructure-Biology. In: Beaufils P., Verdonk R. (eds) *The Meniscus*. Springer, Berlin, 2010, pp.19–27.
30. Leroy A, Beaufils P, Faivre B, et al. Actifit® polyurethane meniscal scaffold: MRI and functional outcomes after a minimum follow-up of 5 years. *Orthop Traumatol Surg Res* 2017; 103(4): 609–614.
31. Sun J, Vijayavenkataraman S and Liu H. An overview of scaffold design and fabrication technology for engineered knee meniscus. *Materials* 2017; 10: 29.
32. Baek J, Chen X, Sovani S, et al. Meniscus tissue engineering using a novel combination of electrospun scaffolds and human meniscus cells embedded within an extracellular matrix hydrogel. *J Orthop Res* 2015; 33(4): 572–583.
33. Mandal BB, Park SH, Gil ES, et al. Multilayered silk scaffolds for meniscus tissue engineering. *Biomaterials* 2011; 32: 639–651.
34. Buma P, van Tienen T and Veth RP. The collagen meniscus implant. *Expert Rev Med Devices* 2007; 4: 507–516.
35. Linke RD, Ulmer M and Imhoff AB. Replacement of the meniscus with a collagen implant (CMI). *Eur J Trauma Emerg Surg* 2007; 33: 435–440.
36. Verdonk R, Verdonk P, Huysse W, et al. Tissue ingrowth after implantation of a novel, biodegradable polyurethane scaffold for treatment of partial meniscal lesions. *Am J Sports Med* 2011; 39: 774–782.
37. Schüttler KF, Pöttgen S, Getgood A, et al. Improvement in outcomes after implantation of a novel polyurethane meniscal scaffold for the treatment of medial meniscus deficiency. *Knee Surgery, Sport Traumatol Arthrosc* 2015; 23(7): 1929–1935.
38. Yan R, Chen Y, Gu Y, et al. A collagen-coated sponge silk scaffold for functional meniscus regeneration. *J Tissue Eng Regen Med* 2019; 13: 156–173.
39. Gruchenberg K, Ignatius A, Friemert B, et al. In vivo performance of a novel silk fibroin scaffold for partial meniscal replacement in a sheep model. *Knee Surgery, Sport Traumatol Arthrosc* 2015; 23(8): 2218–2229.
40. Baker BM, Shah RP, Silverstein AM, et al. Sacrificial nanofibrous composites provide instruction without impediment and enable functional tissue formation. *Proc Natl Acad Sci USA* 2012; 109(35): 14176–14181.
41. Esposito AR, Moda M, Cattani SMDM, et al. PLDLA/PCL-T scaffold for meniscus tissue engineering. *Biores Open Access* 2013; 2(2): 138–147.
42. Gao S, Chen M, Wang P, et al. An electrospun fiber reinforced scaffold promotes total meniscus regeneration in rabbit meniscectomy model. *Acta Biomater* 2018; 73: 127–140.
43. Wood DJ, Minns RJ and Strover A. Replacement of the rabbit medial meniscus with a polyester-carbon fibre bioprosthesis. *Biomaterials* 1990; 11: 13–16.
44. Naal FD, Schauwecker J, Steinhauser E, et al. Biomechanical and immunohistochemical properties of meniscal cartilage after high hydrostatic pressure treatment. *J Biomed Mater Res – Part B Appl Biomater* 2008; 87(1): 19–25.
45. Martinek V, Usas A, Pelinkovic D, et al. Genetic engineering of meniscal allografts. *Tissue Eng* 2002; 8(1): 107–17.
46. Sandmann GH, Eichhorn S, Vogt S, et al. Generation and characterization of a human acellular meniscus scaffold for tissue engineering. *J Biomed Mater Res – Part A* 2009; 14: 324.
47. Maier D, Braeun K, Steinhauser E, et al. In vitro analysis of an allogenic scaffold for tissue-engineered meniscus replacement. *J Orthop Res* 2007; 25: 1598–1608.
48. Chen Y, Chen J, Zhang Z, et al. Current advances in the development of natural meniscus scaffolds: innovative approaches to decellularization and recellularization. *Cell Tissue Res* 2017; 370: 41–52.
49. Sandmann GH, Adamczyk C, Garcia EG, et al. Biomechanical comparison of menisci from different

species and artificial constructs. *BMC Musculoskelet Disord* 2013; 14–324.
50. Porzionato A, Stocco E, Barbon S, et al. Tissue-engineered grafts from human decellularized extracellular matrices: a systematic review and future perspectives. *Ijms* 2018; 19: 4117.
51. Vedi V, Williams A, Tennant SJ, et al. Meniscal movement. An in-vivo study using dynamic MRI. *J Bone Jt Surg - Ser B* 1999; 81(1): 37–41.
52. Kawamura S, Lotito K and Rodeo SA. Biomechanics and healing response of the meniscus. *Oper Tech Sports Med* 2003; 11(2): 68–76.
53. Kaleka CC, Debieux P, Da Costa Astur D, et al. Updates in biological therapies for knee injuries: Menisci. *Curr Rev Musculoskelet Med* 2014; 7: 247–255.
54. Diehl P, Steinhauser E, Gollwitzer H, et al. Biomechanical and immunohistochemical analysis of high hydrostatic pressure-treated achilles tendons. *J Orthop Sci* 2006; 11(4): 380–5.
55. Lichtenberg A, Tudorache I, Cebotari S, et al. Preclinical testing of tissue-engineered heart valves re-endothelialized under simulated physiological conditions. *Circulation* 2006; 114: I-559–I-565.
56. Lovati AB, Bottagisio M and Moretti M. Decellularized and engineered tendons as biological substitutes: a critical review. *Stem Cells Int* 2016; 2016: 7276150.
57. Caddeo S, Boffito M and Sartori S. Tissue engineering approaches in the design of healthy and pathological in vitro tissue models. *Front Bioeng Biotechnol* 2017; 5: 40.
58. Hillebrandt KH, Everwien H, Haep N, et al. Strategies based on organ decellularization and recellularization. *Transpl Int* 2019; 32(6): 571–585.
59. Fu RH, Wang YC, Liu SP, et al. Decellularization and recellularization technologies in tissue engineering. *Cell Transplant* 2014; 23: 621–630.
60. Kuna VK, Xu B and Sumitran-Holgersson S. Decellularization and recellularization methodology for human saphenous veins. *J Vis Exp* 2018; (137): 57803.
61. Yamasaki T, Deie M, Shinomiya R, et al. Transplantation of meniscus regenerated by tissue engineering with a scaffold derived from a rat meniscus and mesenchymal stromal cells derived from rat bone marrow. *Artif Organs* 2008; 32(7): 519–24.
62. Wilson CG, Nishimuta JF and Levenston ME. Chondrocytes and meniscal fibrochondrocytes differentially process aggrecan during de novo extracellular matrix assembly. *Tissue Eng – Part A* 2009; 15(7): 1513–1522.
63. Brown BN, Buckenmeyer MJ, Prest TA. Preparation of Decellularized Biological Scaffolds for 3D Cell Culture. In: Koledova Z. (eds) *3D Cell Culture. Methods in Molecular Biology*, vol 1612. Humana Press, New York, 2017, pp. 15–27.
64. Barbero A, Grogan S, Schäfer D, et al. Age related changes in human articular chondrocyte yield, proliferation and post-expansion chondrogenic capacity. *Osteoarthr Cartil* 2004; 12(6): 476–484.
65. Donnelly H, Salmeron-Sanchez M and Dalby MJ. Designing stem cell niches for differentiation and self-renewal. *J R Soc Interface* 2018; 15: 20180388.
66. Ding Z and Huang H. Mesenchymal stem cells in rabbit meniscus and bone marrow exhibit a similar feature but a heterogeneous multi-differentiation potential: Superiority of meniscus as a cell source for meniscus repair evolutionary developmental biology and morphology. *BMC Musculoskelet Disord* 2015; 16: 65–79.
67. Diaz-Rodriguez P, Chen H, Erndt-Marino JD, et al. Impact of select sophorolipid derivatives on macrophage polarization and viability. *ACS Appl Bio Mater* 2019; 2 (1): 601–612.
68. Chakraborty J, Roy S and Ghosh S. Regulation of decellularized matrix mediated immune response. *Biomater Sci* 2020; 8: 1194–1215.
69. Fontenot AP, Simonian P. Adaptive Immunity, In: Broaddus VD, Mason RJ, Ernst JD, et al. (eds) *Murray and Nadel's Textbook of Respiratory Medicine* 6th ed. W.B. Saunders, 2016, pp. 206–224.
70. Nikbakht M, Pakbin B and Nikbakht Brujeni G. Evaluation of a new lymphocyte proliferation assay based on cyclic voltammetry; an alternative method. *Sci Rep* 2019; 9: 1–8.
71. Greene N, Aleo MD, Louise-May S, et al. Using an in vitro cytotoxicity assay to aid in compound selection for in vivo safety studies. *Bioorganic Med Chem Lett* 2010; 20 (17): 5308–5312.
72. Chew E, Prakash R and Khan W. Mesenchymal stem cells in human meniscal regeneration: a systematic review. *Ann Med Surg (Lond)* 2017; 24: 3–7.
73. Huang Z, Godkin O and Schulze-Tanzil G. The challenge in using mesenchymal stromal cells for recellularization of decellularized cartilage. *Stem Cell Rev Rep* 2017; 13: 50–67.
74. Chen JL, Duan L, Zhu W, et al. Extracellular matrix production in vitro in cartilage tissue engineering. *J Transl Med* 2014; 12: 88.